Deposition and characterization of PbO–PbS multilayer thin films by solution growth technique

Dominic EYA[*]

Department of Physics, Federal University of Technology, Owerri, Nigeria

Abstract: PbO–PbS thin films were deposited on glass substrates using the chemical bath deposition (CBD) technique. PbO thin films were deposited from the solution of lead nitrate $(Pb(NO_3)_2)$ and sodium hydroxide (NaOH). Ethylene-diaminetetraacetate (EDTA) served as the complexing agent. Some of the PbO films were used as substrate for the deposition of PbS. The PbS was deposited from alkaline solution of lead nitrate and thioacetamide. Triethanolamine was used as the complexing agent. Some of the films were subjected to thermal treatment after deposition.

Energy dispersive X-ray fluorescence analysis confirmed the presence of Pb and S in the PbS thin films, while Rutherford backscattering was used to identify the composition of PbO thin films.

The absorbance of PbO–PbS films was extremely high in the UV region and decreased exponentially with increase in wavelength. The transmittance increased sharply but almost linearly with wavelength from the mid-vis region, having a maximum percentage value of 21% at 1000 nm (NIR). Hence, PbO–PbS films are good materials for UV filters and glazing for creating warmth in rooms.

The band gap of PbO–PbS films is in range 2.15–2.25 eV.

Key words: PbO–PbS, chemical bath deposition, thin film, annealing, multilayer, band gap

1. Introduction

Multilayer coating is one way of achieving band gap tuning in semiconductor materials and hence the development of new materials for efficient photovoltaic applications [1].

Thin films are of particular interest for the fabrication of large area arrays, solar selective coatings, solar cells, photoconductors, sensors, antireflection coatings, interference items, polarizer, narrow band filters, IR detectors, waveguide coatings, temperature control of satellites, photothermal solar coatings, magnetic and superconducting films, microelectronic devices etc. [2–5].

Lead sulfide (PbS) is an important semiconductor with a direct narrow band gap of 0.4 eV at 300 K and a relatively large excitation Bohr radius of 18 nm [6,7]. These properties make PbS very suitable for applications as photodetector for IR radiation [6] and other IR detection applications [7,8–15]. The photoresponse depends on the grain size and the topography of the film [16]. Other areas of application include photo resistance [7,17], diode lasers, humidity and temperature sensors [7,18], and decorative and solar control coatings [7,12,18–20]. PbS is also applied for mid-IR lasers, is a good photo catalyst, and has great potential as quantum dots [11].

A number of techniques have been used by various authors to deposit PbS thin films including spray

---

[*]Correspondence: eyadom2003@yahoo.com

pyrolysis [18], sol-gel [21], and chemical bath deposition [8,10,15,17,19]. Chemical bath deposition (CBD) was adopted in the present study. The advantages of the technique have been given previously. The common deposition mechanisms in CBD are the cluster mechanism and the ion-by-ion mechanism. The latter mechanism is the basis of film deposition in this work. Each deposition mechanism has a characteristic growth rate, grain size, and shape that directly affect the nature and properties of the films. Substrates often have a noticeable influence on the film morphology and microstructure and consequently on the electrical and optical properties of the films.

Variation in the deposition parameters, such as temperature and reagent concentrations, allows control of the deposition reaction rates, solubility, and convention and this affects the structural and optical properties of the resulting films. Metal sulfides have a wide range of refractive indices that vary from as low as 1.6 to as high as 5 [8,12,22, http://www.sopra-sa.com/more/database.asp].

On the other hand, lead oxide (PbO) is another direct band gap material whose band gap is within the range 2.0–3.0 eV as reported by various authors [23–25]. It has been applied in the moderation of the structural and optical properties of borate and borosilicate glasses [26,27]. When used to compensate for the lead losses in lead lanthanum titanate (PLT), it creates a ferroelectric domain pinning effect [28].

In this paper, the optical properties of PbO–PbS are investigated and reported on.

2. Experimental details

2.1. Sample preparation

CBD was employed in the deposition of the PbO–PbS thin films. PbO thin films were first deposited on glass substrate from the solution of lead nitrate ($Pb(NO_3)_2$) and sodium hydroxide (NaOH). Ethylenediaminetetraacetate (EDTA) served as the complexing agent. The solution was made in a 50-mL beaker and a 76 mm $\times$ 26 mm $\times$ 1 mm glass slide was used as substrate. Deposition parameters especially reagent concentrations and period of deposition were varied to optimize them. The range of optimum concentration of the reagents used is 0.04 M–0.10 M. Throughout the process 0.10 M of EDTA was used. The optimum period of deposition was 6–18 h.

Later, some samples of PbO were used as substrates for the deposition of PbS. In this case, $Pb(NO_3)_2$ and thioacetamide (CH_3CSNH_2) were used as precursors for Pb^{2+} and S^{2-} ions, respectively. Triethanolamine (TEA) was used as complexing agent while ammonia (NH_3) was used to raise the pH value to alkaline. The reaction of the bath constituents, $Pb(NO_3)_2$ and CH_3CSNH_2, took place in alkaline medium. Again, the reaction parameters were optimized. In this study 0.05 M solutions of $Pb(NO_3)_2$ and CH_3CSNH_2, 1 M solution of TEA, and NH_3 as supplied (88% purity) were used. Twenty milliliters of $Pb(NO_3)_2$ was put in a 50-mL beaker followed by 1 mL of TEA, 1 mL of NH_3, and 20 mL of CH_3CSNH_2. The solution was adequately stirred after each addition. The substrate, supported by synthetic foam cut to shape, was inserted vertically in the solution without allowing it to touch the sides of the beaker. The optimum period of deposition was 2.5–4 h. Some samples of films prepared were annealed at 150 °C.

2.2. Sample characterization

Measurements for the optical characterization of the films were made using a scanning single beam UNICAM Heλ 105 α spectrophotometer in the wavelength range 195 nm–1000 nm.

The compositions of the films deposited were analyzed using energy dispersive X-ray fluorescence (EDXRF). The source uses a silver (Ag) X-ray tube (2.6 keV–20.0 keV) as the excitation source.

EDXRF is a nondestructive method for the elemental analysis of solids and liquids. It is a well-recognized method for the qualitative and quantitative determination of major and minor elements in a wide range of samples.

When materials are exposed to short-wavelength X-rays, ionization of their component atoms may take place. X-rays can be energetic enough to expel tightly held electrons from the inner orbital of the atom. The removal of an electron in this way renders the electronic structure of the atom unstable, and electrons in higher orbital "fall" into the lower orbital to fill the hole left behind. In falling, energy is released in the form of a photon, the energy of which is equal to the energy difference of the 2 orbital involved. Thus, the material emits radiation, which has energy characteristic of the atoms present. The fluorescent radiation can be analyzed by sorting the energies of the photons (energy-dispersive analysis). The intensity of each characteristic radiation is directly related to the amount of each element in the material [www.http://en.wikipedia.org/wiki/x-ray-fluorescence].

In view of the position of oxygen in the periodic table in relation to the excitation source, EDXRF is not suitable for the analysis of the composition of oxide films. Rutherford backscattering (RBS) was used instead for the elemental analysis of PbO thin films.

The structural properties of PbO films were also investigated using a PW1800 X-ray diffractometer with Cu anode.

3. Results and discussion

The first stage of the CBD process is to optimize the deposition parameters such as concentration of reagents, pH of the reaction medium, and the period of deposition. Subsequent depositions are then made at the optimum values. These optimum values are temperature dependent. For the present work, the depositions were carried out at room temperature and the optimized values of the parameters are as stated in section 2.1 above.

The initial films that results from the process of CBD of PbO at room temperature is $Pb(OH)_2$. When these films are thermally treated, we obtain PbO. The range of the annealing temperature for the oxide films is 403–523 K.

The EDXRF of PbO films was able to identify Pb as a constituent of the films by showing the intensity of
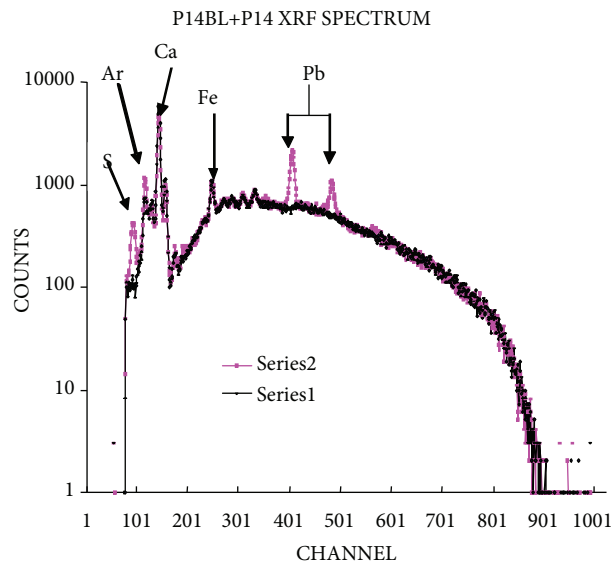

Figure 1. Composition of lead sulfide sample (EDXRF).

Pb, 2.673 c/s in the films but could not however identify oxygen because of its relative position in the periodic table. RBS analysis of the films however showed the films of being composed of 4% Pb and 96% oxygen. Figure 1 also shows EDXRF analysis of the PbS thin films on glass substrate (without and with the films respectively). The result of the EDXRF analysis showed that the plane glass substrate was composed of argon (Ar), calcium (Ca), iron (Fe), arsenic (As), potassium (K), titanium (Ti), manganese (Mn), nickel (Ni), zinc (Zn), and small concentration of copper (Cu), while Pb and S were introduced by the PbS film. The molar ratio for Pb:S was 1:1, indicating PbS.

From the RBS analysis, the film thickness for PbO was 150 nm. On the other hand, the range of thickness of the PbS films deposited was on average 493–837 nm.

The X-ray diffraction (XRD) of PbO and the detailed analysis of the crystal structure based on the result have been discussed in an earlier paper [24]. According to the analysis, the structure of PbO films is strongly temperature dependent. The films as deposited at 300 K (room temperature) show distinct peaks at the diffraction planes (100), (110), and (111). For films annealed at 403 K, the numbers of peaks increased and are at (110), (011), (200), (020), and (002). On increasing the annealing temperature to 463 K, the peaks reduce to one broad peak at (111) diffraction plane. Annealing the films at 503 K, the structure returns to almost the same as those of unannealed films at 300 K.

The grain sizes, D, corresponding to the various diffraction peaks were estimated by Scherrer's formula:

$$D = \frac{K\lambda_x}{\beta \cos\theta} \tag{1}$$

where K is a dimensionless constant (0.9), the diffraction angle is 2θ, λ_x is the X-ray wavelength, and β is the full width at half maximum (FWHM) of the diffraction peak. The values obtained are shown in the Table.

Table. Grain size of PbO thin films under various thermal treatments and diffraction peaks.

Diffraction peaks	D values for PO$_1$-T$_R$ (nm)	D values for PO$_p$-T$_{403K}$ (nm)	D values for PO$_3$-T$_{463K}$ (nm)
100	0.696	-	-
110	-	0.709	-
110	0.412	-	-
011	-	0.413	-
111	0.363	-	-
111	-	0.468	-
111	-	0.987	-
200	-	0.509	-
020	-	0.519	-
002	-	0.396	-
200	-	0.406	-
200	-	0.409	-
111	-	-	0.097

The absorbance of PbO–PbS is infinitely large in the UV region and greater than 1 throughout the vis region. The minimum value is 0.872 in the near IR (NIR) (940 nm) region. It has an exponential decay pattern as shown in Figure 2. This shows that the absorbance is very large up to the NIR region of the electromagnetic spectrum. In their separate analysis in earlier papers, the absorbance of PbS thin films falls from a very high value in the UV region to about 0.12 in the NIR region. PbO has a similar trend of absorbance [8,24].

Within the UV and the first half of the vis region, the transmittance of PbO–PbS films is negligible. The transmittance, however, increased almost linearly with wavelength from 440 nm into the IR region as shown in Figure 3. The trend is similar in both PbO and PbS thin films but the rate is sharper in PbO–PbS films. Despite the linear increase, the percentage transmittance remains low (14.4%–21.0% at a wavelength of 1000 nm), resulting from the very high absorbance throughout the various regions of the electromagnetic spectrum and diffuse reflection from the surface of the films [7]. PbS has peak optical transmittance in the NIR region as 54.5%, while the value for PbO is about 75.0% [8,24].
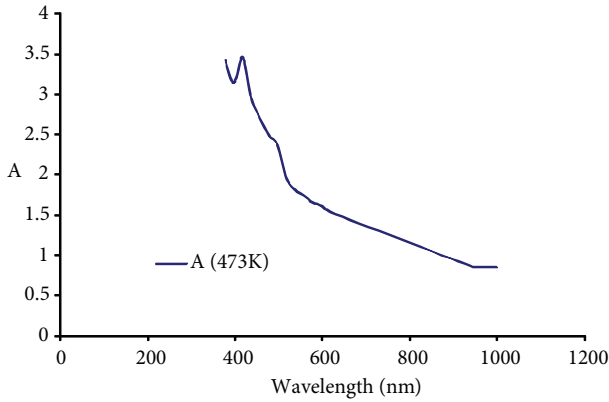

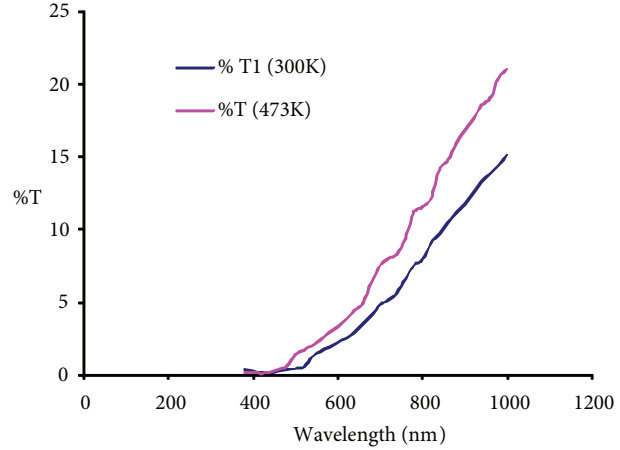**Figure 2.** A graph of absorbance, A, versus wavelength for PbO–PbS thin films.

Figure 3. A graph of transmittance, %T, versus wavelength for PbO–PbS thin film samples at 300 K and annealed at 473 K.

The optical properties of semiconductor materials are related by

$$A + T + R = 1 \tag{2}$$

where A is absorbance of the film, T the transmittance, and R the reflectance. The relation enables the evaluation of R since A and T were obtained experimentally. One observes that the value of A is greater than 1 up to the NIR region. The evaluation of R in this situation will be erroneous as it will result in negative values.

It has been identified that PbO–PbS is direct band gap semiconductor and for direct allowed transition the absorption coefficient is given by [29]

$$\alpha = \frac{(hv - Eg)^{1/2}}{hv} \tag{3}$$

The optical band gap is obtained by extrapolating the linear portion of the plot $(\alpha hv)^2$ versus hv to $\alpha = 0$ as shown in Figure 4. The range of band gap obtained for PbO–PbS thin films is 2.15–2.25 eV. In previous papers, band gap ranges of 1.85–2.60 eV and 2.00–3.00 eV were reported for PbS and PbO respectively [8,25].

The extinction coefficient, k, of the material is given by

$$k = \frac{\alpha\lambda}{4\pi} \tag{4}$$

The spectral variation in the extinction coefficient of the PbO–PbS films is shown in Figure 5. The extinction coefficient rises to peak (0.24, 0.23 at 440 nm) at the beginning of the vis region and decreases exponentially with increasing wavelength.
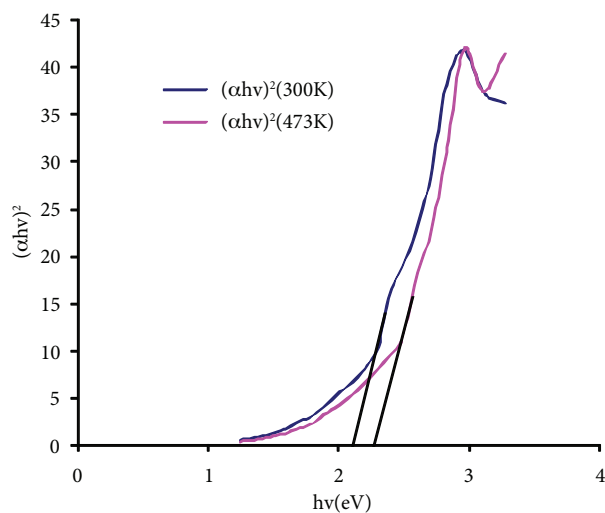
Figure 4. A graph of $(\alpha\,hv)^2$E13 $(eV^2\,m^{-2})$ versus hv for PbO–PbS thin film samples at 300 K and annealed at 473 K.
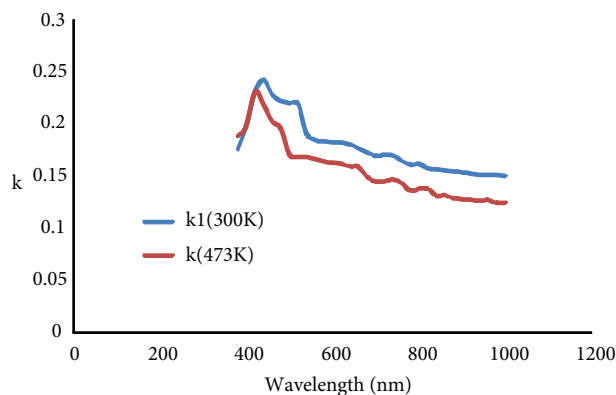
Figure 5. A graph of extinction coefficient, k versus wavelength for PbO–PbS thin film samples at 300 K and annealed at 473 K.

4. Conclusion

PbO–PbS thin films have been successfully deposited on glass substrate by CBD. The films have very high absorbance from UV to NIR regions. The transmittance increases sharply with increase in wavelength from the mid-vis region. The material has potential application in UV filters and glazing for creating warmth in rooms. The band gap of the films is in the range of 2.15–2.25 eV.

References

[1] Ezema, F. I.; Hile, D. D.; Ezugwu, S. C.; Osuji, R. U.; Asogwa, P. U. *J. Ovonic Res.* **2010**, *6*, 99–104.

[2] Eya, D. D. O.; Eze, F. C. *Nig. J. Phys.* **2011**, *22*, 63–73.

[3] Pathan, H. M.; Lokhande, C. D. *Bull. Mater. Sci.* **2004**, *27,* 85–111.

[4] Sukyte, J.; Janickis, V.; Ivanauskas, R.; Zalenkiene, S. *Mater. Sci. MEDZIAGOTYRA).* **2007**, *13,* 33–38.

[5] Mane, R. S.; Lokhande, C. D. *Mater. Chem. Phys.* **2000**, *65,* 1–31.

[6] Popescu, V.; Popescu, G. L.; Moldovan, M.; Preimerean, C. *Chalcogenide Letters* **2009**, *6,* 503–508.

[7] Seghaier, S.; Kamoun, N.; Brini, R.; Amara, A. B. *Mat. Chem. Phys.* **2006**, *97*, 71–80.

[8] Eya, D. D. O.; Eze, F. C. *Nig. J. Phys.* **2009**, *21,* 10–20.

[9] Yang, Y.J.; Hu, S. *Thin Solid Films.* **2008**, *516,* 6048–6051.

[10] Fernandez-Lima, F. A.; Gonzalez-Alfaro, Y.; Larramendi, E. M.; Fonseca-Filho, H. D.; Maia da Costa, M. E. H.; Freire, Jnr, F. L.; Prioli, R.; de Avillez, R. R.; da Silveira, E.F.; Calzadilla, O.; et al. *Mater. Sci. Eng. B.* **2007**, *136,* 187–192.

[11] Rempel, A. A.; Kozhevnikova, N. S.; Leenaers, A. J. G.; Vanden Berghe, S. *J. Cryst. Growth* **2005**, *280*, 300–308.

[12] Osherov, A.; Ezersky, V.; Golan, Y. *J. Cryst. Growth* **2007**, *308*, 334–339.

[13] Ndukwe, I. C. *Nig. J. Phys.* **1998**, *10*, 7–11.

[14] Amusan, J. A.; Fajinmi, G. R.; Sanus, Y. K. *Res. J. Appl. Sci.* **2007**, *2*, 931–934.

[15] Choudhury, N.; Sarma, B. K. *Ind. J. Pure & Appl. Phys.* **2008**, *46*, 261–265.

[16] Larramendi, E. M.; Calzadilla, O.; González-Arias, A.; Hernández, E.; Ruiz- Garcia. J. *Thin Solid Films* **2001**, *389*, 301–306.

[17] Pentia, E.; Pintilie, L.; Matei, I.; Botila, T.; Ozbay, E. *J. Optoelectron. Adv. M.* **2001**, *3*, 525–530.

[18] Popeseu, V.; Nasai, H. I.; Darvasi, E. *J. Optoelectron. Adv. M.* **2006**, *8*, 1187–1193.

[19] Yang, Y. J.; Hu, S. *Thin Solid Films* **2008**, *516*, 6048–6051.

[20] Pop, I.; Nascu, C.; Ionescu, V.; Indrea, E.; Bratu, I. *Thin Solid Films* **1997**, *307*, 240 – 244.

[21] Wang, X.; Shi, J.; Yang, Y. *J. Appl. Phys.* **2004**, *95*, 4791.

[22] Gopal, V.; Harrington, J. A. *Optics Express* **2003**, *11*, 3182.

[23] Nwodo, M. O.; Ezugwu, S.C.; Ezema, F. I.; Osuji, R. U.; Asogwa, P. U. *J. Optoelectron. Biomed. Mater.* **2011**, *3*, 95–100.

[24] Eya, D. D. O. *Pacific Journal of Science and Technology* **2006**, *7*, 114–119.

[25] Harris, E. P.; Hauge, P. S.; Kircher, C. J. *Applied Physics Letters* **1979**, *34*, 680–682.

[26] Singh, D.; Singh, K.; Singh, G.; Manupriya, S.; Mohan, M.; Sharma, G. *J. Phys. Condens. Matter.* **2008**, *20*, 075228–075228.

[27] Shajo, S.; Khadar, M. A. *Bull. Mater. Sci.* **2004**, *27*, 207–212.

[28] Song, Z.; Ren, W.; Wang, S.; Wang, L.; Lin, C.; Zhang, L.; Yao, X. *J. Phys. D: Appl. Phys.* **2000**, *33*, 764–772.

[29] Narayanan, K. L.; Vijayakumar, K. P.; Nair, K. G. M.; Thampi, N. S.; Krishan, K. *J. Mater. Sci.* **1997**, *32*, 4837–4840.